Nitrous oxide emissions from two full-scale membrane-aerated biofilm reactors

Nerea Uri-Carreño[a,b,*], Per H. Nielsen[a], Krist V. Gernaey[b], Carlos Domingo-Félez[b], Xavier Flores-Alsina[b]

[a] Vandcenter Syd A/S, Vandværksvej 7, Odense, 5000, Denmark

[b] Process and Systems Engineering Center (PROSYS), Department of Chemical and Biochemical Engineering, Technical University of Denmark, Søltofts Plads 228A, Kgs. Lyngby, 2800, Denmark

* Corresponding author: nur@vandcenter.dk

Abstract

The upcoming change of legislation in some European countries where wastewater treatment facilities will start to be taxed based on direct greenhouse gas (GHG) emissions will force water utilities to take a closer look at nitrous oxide (N_2O) production. In this study, we report for the first time N_2O emissions from two full-scale size membrane aerated biofilm reactors (MABR) (R1, R2) from two different manufacturers treating municipal wastewater. N_2O was monitored continuously for 12 months in both the MABR exhaust gas and liquid phase. Multivariate analysis was used to assess process performance. Results show that emission factors (EF_{N2O}) for both R1 and R2 (0.88±1.28 and 0.82±0.86%) were very similar to each other and below the standard value from the Intergovernmental Panel on Climate Change (IPCC) 2019 (1.6%). More specifically, N_2O was predominantly emitted in the MABR exhaust gas (NTR_{exh}) and was strongly correlated to the ammonia/um load ($NH_{x,load}$). Nevertheless, the implemented

Oxidation Reduction Potential (ORP) control strategy increased the bulk contribution (NTR_{bulk}), impacting the overall EF_{N2O}. A thorough analysis of dynamic data reveals that the changes in the external aeration (EA)/loading rate patterns suggested by ORP control substantially impacted N_2O mass transfer and biological production processes. It also suggests that NTR_{exh} is mainly caused by ammonia-oxidizing organisms (AOO) activity, while ordinary heterotrophic organisms (OHO) are responsible for NTR_{bulk}. Different methods for calculating EF_{N2O} were compared, and results showed EF_{N2O} would range from 0.6 to 5.5 depending on the assumptions made. Based on existing literature, a strong correlation between EF_{N2O} and nitrogen loading rate (R^2 = 0.73) was found for different technologies. Overall, an average EF_{N2O} of 0.86 % N_2O-N per N load was found with a nitrogen loading rate greater than 200 g N m^{-3} d^{-1}, which supports the hypothesis that MABR technology can achieve intensified biological nutrient removal without increasing N_2O emissions.

Keywords

Biofilm, IFAS, MABR, N_2O, process intensification

Nomenclature

A	Membrane surface area, m^2
AOO	Ammonia oxidizing organism
AP	Abiotic pathway
BNR	Biological nutrient removal
C/N ratio	Ratio of soluble chemical oxygen demand and ammonia/um
$C_{N2O,air}$	Nitrous oxide concentration measured in atmosphere, ppm
$C_{N2O,bulk}$	Nitrous oxide concentration measured in bulk, g N m^{-3}
$C_{N2O,exh}$	Nitrous oxide concentration measured in exhaust, ppm
$C_{O2,in/out}$	Oxygen concentration in atmospheric air and exhaust gas after membranes, %
EA	External aeration, final bubble aeration in R1 and fine bubble + coarse bubble in R2
EF_{N2O}	Nitrous oxide emission factor, % N load emitted as N_2O-N
$EF_{N2O,sc2}$	Nitrous oxide emission factor including liquid emissions, % N load emitted as N_2O-N

$EF_{N2O,\Delta NH}$	Nitrous oxide emission factor, % ammonia/um nitrogen removal emitted as N_2O-N
$EF_{N2O,OTR}$	Nitrous oxide emission factor based on OTR-calculated NR, % ammonia/um nitrogen removal emitted as N_2O-N
f_{org}	Ammonia-total nitrogen conversion constant
GHG	Greenhouse gas
H_{N2O}	Henry's law coefficient, -
HD	Heterotrophic denitrification pathway
IPCC	Intergovernmental Panel on Climate Change
$K_La_{N2O,aer}$	Mass transfer coefficient when EA was on, d^{-1}
$K_La_{N2O,un}$	Mass transfer coefficient when EA was off, d^{-1}
MABR	Membrane-aerated biofilm reactor
N	Nitrogen
N_{N2O}	Nitrous oxide mass, g N
N_2O	Nitrous oxide
ND	Nitrifier-denitrification pathway
$NH_{x,inf/eff}$	Ammonia/um concentration in the influent/effluent, g N m^{-3}
$NH_{x,load}$	Ammonia/um load in influent, kg N d^{-1}
NLR	Nitrogen loading rate, g N m^{-3} d^{-1}
NN	Nitrifier-nitrification pathway
NR	Nitrification rate, g N m^{-2} d^{-1}
NTR_{exh}	Gaseous nitrous oxide transfer rate in MABR exhaust, g N d^{-1}
$NTR_{bulk,aer}$	Gaseous nitrous oxide transfer rate in bulk mixed liquor when external aeration on, g N d^{-1}
$NTR_{bulk,liq}$	Liquid nitrous oxide emission, g N d^{-1}
$NTR_{bulk,un}$	Gaseous nitrous oxide transfer rate in bulk mixed liquor when external aeration off, g N d^{-1}
$NTR_{bulk,sc2}$	Nitrous oxide transfer rate including gaseous and liquid emission, g N d^{-1}
OHO	Ordinary heterotrophic organism
ORP	Oxidation- Reduction Potential, mV
OTR	Oxygen transfer rate, g O_2 m^{-2} d^{-1}
P_{out}	Pressure in exhaust, bar
PCA	Principal Component Analysis
R	Ideal gas constant
R1/R2	MABR 1 and 2
SCADA	Supervisory control and data acquisition
TN_{load}	Total nitrogen load, g N d^{-1}
$Q_{air,in}$	Process airflow, N m^3 d^{-1}
$Q_{air,EA}$	External aeration airflow, m^3 d^{-1}
Q_{inf}	Feed flow to the MABR, m^3 h^{-1}

V	Aerated volume of reactor, m^3
V_{loss}	Volumetric airloss
WRRF	Wastewater and Resource Recovery Facility
ρo_2	Oxygen density under normal conditions, kg m^{-3}

1 INTRODUCTION

Water utilities around the world are setting carbon goals, especially in Denmark, where the country has set the ambitious goal of cutting 70% of its greenhouse gas (GHG) emissions by 2030, and the whole water sector has a common goal of achieving climate neutrality by 2030 (Danish Government, 2020). While some countries' energy-related CO_2 emissions are expected to continue increasing in the coming years (Aydin, 2014), for others, such as Denmark, these are already following a downward trend (Irandoust, 2016). As countries de-carbonize their energy systems, reducing their carbon intensity and thereby reducing indirect emissions, direct emissions will become more critical in the overall carbon balance of a water treatment facility (Delre et al., 2019). Moreover, new GHG emissions regulations, including a tax on nitrous oxide (N_2O) emissions from wastewater treatment plants, could be on their way (Danish Government, 2020).

Data from long-term monitoring of facilities performing biological nutrient removal (BNR) shows, in general, low N_2O emission factors (EF_{N2O}), lower than the "tier 1" value from the Intergovernmental Panel on Climate Change (IPCC) 2019 of 1.6% of the incoming nitrogen (N) load emitted as N_2O-N (Miljøstyrelsen, 2020; Valkova et al., 2021; Vogt et al., 2021; de Haas and Andrews, 2022). Two recent efforts by Denmark and Switzerland to use long-term data from full-scale facilities resulted in a reduction of the national EF_{N2O} ("tier 2") from 1.6 to 0.84% in Denmark (Miljøstyrelsen, 2020) and 0.9% in Switzerland (for full N removal facilities) (Vogt et al., 2021). Novel technologies, however, have been

reported to have generally higher EF_{N2O}, especially those technologies that aim to "intensify" BNR, achieving a higher N removal per m^3 of reactor volume, such as anaerobic digestion supernatant treatment processes (Vasilaki et al., 2019; Valkova et al., 2021). The recents works of Faragò et al., 2021 and Monje et al., 2022, where life cycle and economic assessment evaluations were used to quantify the environmental impacts of retrofitting existing facilities with novel technologies showed that direct N_2O emissions were the most significant contributor to climate change in all scenarios. It is therefore of utmost importance to collect accurate estimations of EF_{N2O} for different technologies.

The membrane aerated biofilm reactor (MABR) technology brings together several aspects beneficial for facilities striving to become energy and carbon-neutral (He et al., 2021). The increased oxygen transfer efficiency reduces energy consumption (Castrillo et al., 2019; Uri-Carreño et al., 2021), while the fixed biofilm increases N removal capacity (Kunetz et al., 2016). When operated in combination with activated sludge (hybrid MABR), it allows for the intensification of BNR facilities (Downing and Nerenberg, 2008), thereby increasing the capacity of the plant and reducing its footprint (Carlson et al., 2021). Moreover, one of the key traits of MABR, its counter-diffusional nature, provides the environmental conditions for simultaneous nitrification and denitrification to occur, and this has been previously identified as an N_2O sink (Conthe et al., 2019). MABR has, therefore, the potential to achieve successful N removal intensification while reducing the direct GHG emissions associated.

Laboratory-scale studies have shown that MABR could have a substantial advantage over conventional technologies regarding N_2O emissions. Kinh et al., 2017 and Pellicer-Nàcher et al., 2010 found in laboratory-scale studies that N_2O emissions were two orders of magnitude lower when performing nitrification-denitrification and autotrophic N removal (respectively) compared to conventional biofilm technologies. However, neither of those studies reported the N_2O fraction that back-diffuses into the

membrane lumen and could significantly change the final N_2O emission mass balance. More recently, Silveira et al., 2022 showed that N_2O concentrations measured in the MABR exhaust from a pilot treating 630 m^3 d^{-1} were, on average, in the 60-120 ppm range and could be used to assess biofilm development during startup. This study, however, did not quantify the emission fraction coming from the bulk.

In this study, we analyze for the first time one year of continuous monitoring data of two full-scale MABRs located in pilot reactors adjacent to the bio-p zones at the Ejby Mølle Water and Resource Recovery Facility (WRRF) (Uri-Carreño et al., 2021). This study goes beyond scientific literature's state of the art by reporting N_2O emissions in both exhaust and bulk from a full-scale size MABR treating municipal wastewater. High-frequency N_2O data is analyzed together with other performance indicators. A discussion of the potential N_2O formation mechanism is included based on dynamic profiles. This study also shows the impact of the statistical methods employed to calculate and report these emissions. Results from this study will help benchmark MABR technology in comparison to other intensification technologies.

2 METHODS

2.1 MABR SYSTEM UNDER STUDY

2.1.1. Pilot description

The Ejby Mølle WRRF in Odense, Denmark, has a 410,000 population equivalents treatment capacity. The main liquid treatment train comprises grit removal and screening (6 mm), chemically enhanced primary treatment with the addition of polymers and ferric sulfate, and Bio-Denipho™ nutrient removal

with phased isolation ditches, including anaerobic zones for biological phosphorus removal. Further details on the plant have been reported by Uri-Carreño et al., 2021.

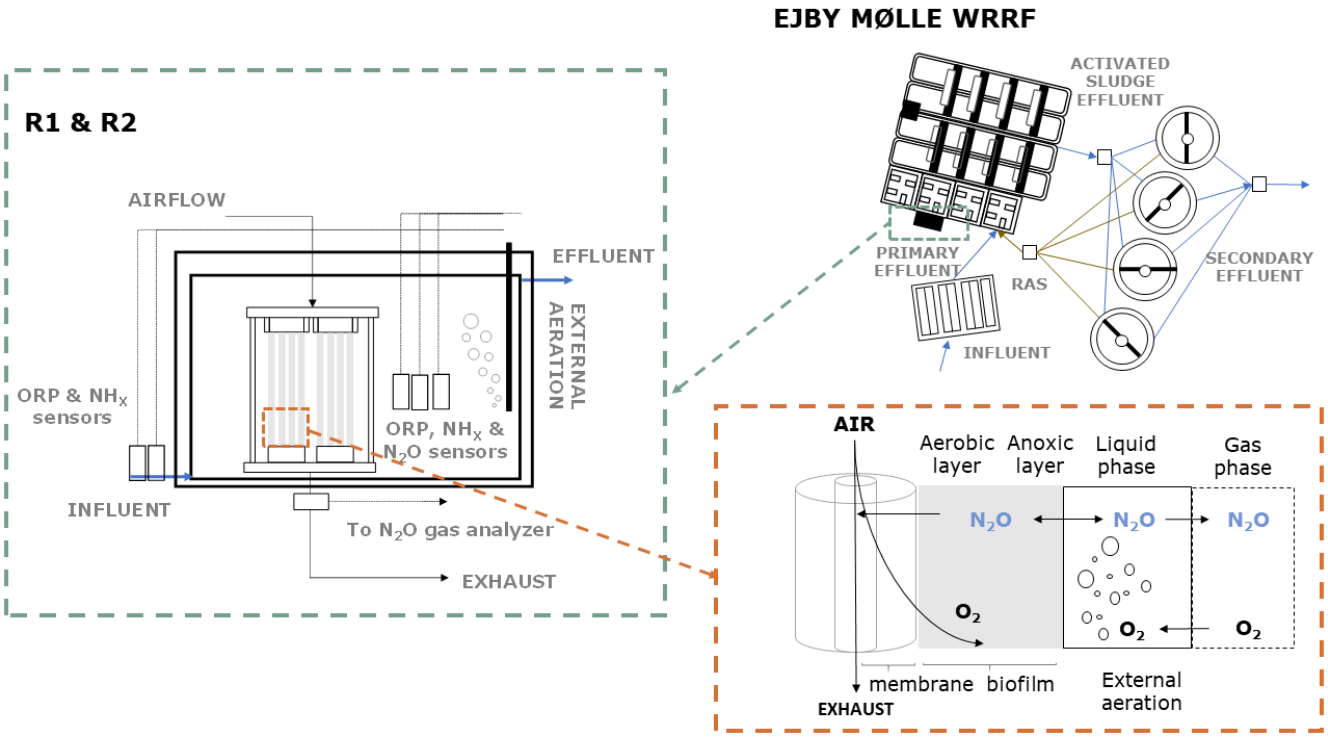

Fig 1. Location of MABR pilot reactors at the Ejby Mølle WRRF on the top right, a detailed schematic of the reactors on the top left, and a closeup of membranes and biofilm on the bottom right.

The MABR tanks consisted of two sidestream circular reactors of 23 m^3 (R1) and 17 m^3 (R2) each, adjacent to the bioreactor facility's anaerobic zone. Two full-scale hollow-fiber MABR cassettes with a total volume of 11.3 m^3 and 4.5 m^3 and a total membrane surface area of 1920 m^2 and 1450 m^2 were installed inside Reactor 1 (R1) and 2 (R2) in 2018, respectively. The reactors were set up as continuously stirred-tank reactors fed with mixed liquor from the full-scale anaerobic zones (i.e., primary effluent mixed with return activated sludge). Low-pressure air was supplied to the MABR units for intramembrane oxygen supply and mixing/scouring.

2.1.2 Operational description – ORP control strategy

An oxidation-reduction potential (ORP)-based control strategy was implemented in the pilot reactors, and external aeration (EA) in the form of fine-bubble diffusers was added to R1 and R2. More specifically, a low value of ORP would trigger the use of EA, and a high value of ORP would stop it. A second layer was added so that if the ORP reached an even lower setpoint (meaning EA was not enough to bring ORP to the desired range of values), it would significantly decrease the feed to the reactor until the defined high ORP setpoint was reached. The ORP control strategy was intended to overcome previous operation problems related to iron sulfide precipitation and sulfide inhibition which is described in more detail in Uri-Carreño et al., 2022.

Biofilm scouring was carried out using coarse bubble aeration in both R1 and R2. This is typically done using short pulses of air. However, coarse bubble aeration was used during extended periods in R2, and it was therefore included in the N_2O stripping calculations as EA (whenever $Q > 312$ m^3 d^{-1}). Therefore, in this study, EA refers to fine bubble aeration in R1 and the combination of fine and coarse bubble aeration in R2.

2.1.1 Data acquisition

NH_x concentrations ($NH_{x,eff}$) and temperature were measured using an AmmoLyt® plus device from Xylem Inc. N_2O concentrations in the liquid phase (bulk) were monitored using a Clark-type sensor from Unisense A/S. A sample from the exhaust gas after the MABR unit was taken semi-continuously to a gas-monitoring GASloq 1200 from ABB Group SA. The system contained a gas analyzer Uras 26 Easyline and was designed to operate as a multi-scan and measuring point analysis system with O_2 and N_2O measurement. The gas analyzer measured one sample at a time, oscillating between R1 and R2

every 24h. Both probes and the gas analyzer were connected to the SCADA system, and measurements were recorded every ten seconds from January until December 2020.

2.2 PROCESS RATE CALCULATIONS

2.2.1 Nitrification and oxygen transfer rates

The oxygen transfer rate (OTR, g O_2 m^{-2} d^{-1}) measures the flux of oxygen gas that diffuses from the lumen's interior into the biofilm over time and was calculated following the exhaust oxygen model in Houweling & Daigger, 2019 (Eq1,2):

$$OTR = \frac{Q_{air,in}\,(C_{o_{2,\,in}} - (1-V_{loss})C_{o_{2,\,out}})\rho_{o_2}}{A} \qquad \text{Eq 1}$$

$$V_{loss} = \frac{1 - C_{o_{2,\,in}}}{1 - C_{o_{2,\,out}}} \qquad \text{Eq 2}$$

Where $Q_{air,in}$ is airflow (N m^3 d^{-1}), $C_{o2,in}$ is the mole fraction of oxygen in atmospheric air, V_{loss} is the volumetric air loss between inlet and outlet, $C_{o2,out}$ is the mole fraction of oxygen in the exhaust. ρ_{o2} is the oxygen density under normal conditions (kg m^{-3}), and A is the membrane surface area (m^2).

Nitrification rates (NR) represent the quantity of NH_x oxidized to NO_x. They were calculated using NH_x concentrations from the NH_x sensor (NR) as in Eq 3 where $NH_{x,inf,}$ and $NH_{x,eff}$ (g m^{-3}) respectively represent the concentration of NH_x in influent and effluent obtained from online signals and Q_{inf} was the influent flow rate (m^3 d^{-1}). More information about process indicators calculation methods can be found

in Uri-Carreño et al., 2021. Note that these nitrification rates include neither the hydrolysis and ammonification nor the biomass assimilation in the system.

$$NR = \frac{\left(NH_{x,inf} - NH_{x,eff}\right) * Q_{inf}}{A} \quad \text{Eq 3}$$

2.2.2 N_2O emissions

2.2.2.1 Gaseous emissions from the bulk mixed liquor

The nitrous oxide transfer rate (NTR_{bulk}) emitted from the bulk mixed liquor surrounding the MABR units (g N d^{-1}) was calculated as the sum of the emissions when EA was on $NTR_{bulk,aer}$, and when it was off: $NTR_{bulk,un}$. The mass transfer coefficient for N_2O, $K_La_{N2O,aer}$, used in Eq 4b was calculated according to Matter-Müller et al., 1981, while a value of 2 d^{-1} was used in Eq 4c. $C_{N2O,\ bulk}$ corresponds to the concentration of N_2O measured in the liquid phase (g N m^{-3}), $C_{N2O,air}$ is the concentration of N_2O in the atmosphere (g N m^{-3}), $Q_{air,EA}$ is the EA airflow (m^3 d^{-1}), estimated based on blower speed, and V is the aerated volume of the reactor, which in this case we assume was 100% of the reactor volume. Measurements below the detection limit (0.005 g N m^{-3}) were assumed to be 0. Liquid NTR from the bulk ($NTR_{bulk,liq}$) was calculated according to Eq 4d, and the NTR, including liquid and gaseous emissions ($NTR_{bulk,sc2}$), was calculated using Eq 4e.

$$NTR_{bulk} = NTR_{bulk,aer} + NTR_{bulk,un} \quad \text{Eq 4a}$$

$$NTR_{bulk,aer} = H_{N_2O} * C_{N_2O}^{bulk} * Q_{air.EA} * \left(1 - e^{-\frac{K_L a_{N_2O,aer}}{H_{N_2O}} * \frac{V}{Q_{air.EA}}}\right) \quad \text{Eq 4b}$$

$$NTR_{bulk,un} = K_L a_{N_2O,un} * \left(C_{N_2O}^{bulk} - \frac{C_{N_2O}^{air}}{H_{N_2O}}\right) * V \quad \text{Eq 4c}$$

$$NTR_{bulk,liq} = C_{N_2O}^{bulk} * Q_{inf} \quad \text{Eq 4d}$$

$$NTR_{bulk,sc2} = NTR_{bulk,aer} + NTR_{bulk,unaer} + NTR_{bulk,liq}$$ Eq 4e

2.2.2.2 Gaseous emissions from the MABR exhaust

The gaseous N_2O emission from the MABR exhaust was calculated based on the concentration of N_2O measured in the exhaust gas, $C_{N2O,exh}$ (ppm) using Eq 5, where NTR_{exh} has units g N d^{-1}. $N_{N2O,exh}$ has units of g N, P_{out} is the pressure in the exhaust gas (bar), $Q_{air,in}$ is the inlet airflow to the MABR units (m^3 d^{-1}), V_{loss} is the estimated volume loss across the MABR units (Eq 2), R is the ideal gas constant, and T is the temperature of the exhaust gas, which in this case is assumed to be equal to the liquid temperature in the MABR tank.

$$NTR_{exh} = \frac{\Delta n_{N2O,exh}}{\Delta t} = \frac{P_{out} * Q_{air,in} * V_{loss} * C_{N2O,exh}}{R * T}$$ Eq 5

2.2.2.3 Emission factor

The N_2O emission factor, EF_{N2O}, was calculated using the sum of the gaseous emissions from the MABRs, divided by the influent N load, TN_{load} (Eq 6a). Since no TN measurements from the inlet to the MABRs were available, only influent NH_x concentrations, we estimated the corresponding TN_{load} using a constant f_{org}, as was also done in van Dijk et al., 2021. F_{org} was estimated using TN and NH_x measurements from the primary effluent and fitting a linear regression model (R^2 = 0.89). $EF_{N2O,sc2}$ includes in the scope of the system the dissolved N_2O that leaves the system with the effluent. $EF_{N2O,\Delta NH}$ corresponds to the N_2O emission factor per NH_x removed in the system, calculated using NHx sensor measurements (Eq 6e), and it has units of % N emitted as N_2O per g of NH_x-N removed. $EF_{N2O,OTR}$ is a variation of the latter, in which NH_x removal is calculated based on OTR through the membranes and the theoretical oxygen demand for nitrification.

$$EF_{N2O} = \frac{(NTR_{bulk} + NTR_{exh}) * 100}{TN_{load}} \quad \text{Eq 6a}$$

$$TN_{load} = \mathrm{NH_{x,inf}} * \mathrm{Q_{inf}} * f_{org} \quad \text{Eq 6b}$$

$$EF_{N2O,sc2} = \frac{(NTR_{bulk,sc2} + NTR_{exh}) * 100}{TN_{load}} \quad \text{Eq 6c}$$

$$\mathrm{EF_{N2O,\Delta NH}} = \frac{(NTR_{bulk} + NTR_{exh}) * 100}{\Delta NHx} \quad \text{Eq 6d}$$

$$\Delta NH_x = NR * A \quad \text{Eq 6e}$$

$$EF_{N2O,OTR} = \frac{(NTR_{bulk} + NTR_{exh}) * 100}{\Delta NHx,\ OTR} \quad \text{Eq 6f}$$

$$\Delta NH_{x,OTR} = OTR/4.57 \quad \text{Eq 6g}$$

2.3 DATA ANALYSIS

The pre-processing of the data included the treatment of missing values and removal of data corresponding to periods when the system was temporarily out of service for different reasons: maintenance of equipment or emptying the reactor tank. All analyses were performed using R software. Results were considered “significant” when the p-value was < 0.05 and "highly significant" when the p-value < 0.001. Shapiro-Wilk tests were carried out to test normality in the data distributions.

The gas analyzer was out of range 4.2% of the time (≥ 324 ppm). Using a Bayesian parameter estimator, we calculated the true mean and standard deviations (including values out of range) for the concentration of N_2O in the exhaust. The mean and standard deviation of uncorrected data were 152.3±94.1 and 88.3±86.0 for R1 and R2, while the estimated true mean and standard deviations were 154.3±98.9 and 89.0±88.0. Therefore, we conclude that the time the gas analyzer was out of range did not affect our results significantly. Eliminating the values out of range (324 ppm) prior to the PCA analysis showed no differences in the results.

The error from the NH_x sensors was reduced by eliminating periods where the difference between laboratory and sensor measurements was > 3 g N m^{-3}. In March 2020, due to COVID lockdowns in Denmark, the NH_x sensors could not be appropriately maintained, and therefore NH_x online data was excluded for EF_{N2O} calculations (both R1 and R2). In early June 2020, a chemical cleaning was carried out in R2 (which is better described in Uri-Carreño et al., 2022), and the three weeks of operation following that chemical cleaning were deemed as "startup period" and were left out of the EF_{N2O} calculations.

The dissolved N_2O sensor is susceptible to temperature changes (Jenni et al., 2012), and we observed deviations from the baseline zero concentration over time between calibrations (positive and negative deviations). The data set was adjusted to account for these deviations by increasing or reducing all measured values. The dissolved N_2O sensor measures linearly in the 0.005-1.5 g N m^{-3} range. To account for the low measurement range, we assumed that concentrations < 0.005 mg N m^{-3} were 0, which means the minimum NTR that could be measured above the detection limit was 5.5 g N d^{-1}, which corresponds to an EF_{N2O} of 0.1% (using average annual load). Measurements above the measurement range (1.5 g N m^{-3}) were not eliminated from the data set. The behavior of the Clark-type sensor above the measurement range suggests the emissions during these periods (0.54% of the data set) are underestimated.

2.3.1 PCA

A multivariate analysis of the sensors/gas analyzers data was performed using principal component analysis (PCA). PCA extracted the eigenvalues from the covariance matrix of the scaled and centered variables. The PCs are the uncorrelated (orthogonal) variables obtained by multiplying the original correlated variables with the eigenvectors. Each eigenvector consists of a vector of coefficients (loadings). PCA allowed reducing the dimensionality of the original data set with a minimum loss of

209 information. The selection of the PCs was based on eigenvalues > 1. A Promax rotation was performed

210 on the PC eigenvalues to achieve a simpler, easier to interpret structure.

211 2.3.2 N_2O emissions reporting

212 Six different scenarios with different ways of reporting EF_{N2O} were defined (see Table 1).

213 **Table 1.** Description of EF_{N2O} calculations.

Scenario	Description
SC1	Exhaust and bulk gaseous emissions and the estimated **load** to the MABRs based on **NH_x sensors** (see eq 6a).
SC2	Equal to SC1 with the addition of the N_2O emissions from the **bulk liquid** leaving the pilot with the effluent (see Eq 4d, 6c)
SC3	Exhaust and bulk gaseous emissions and the estimated NHx **removal** in the MABRs based on **NH_x sensors** (see eq 6d, 6e).
SC4	Exhaust and bulk gaseous emissions and the estimated NHx **removal** in the MABRs based on **OTR** (see eq 6f, 6g).
SC5	Exhaust and bulk gaseous emissions and the estimated **load** to the MABRs based on **laboratory** analysis of NH_x (see eq 6a).
SC6	Same as SC1, using the **90^{th} percentile.**

214

215

3 RESULTS

3.1 PLANT PERFORMANCE AND OVERALL EF_{N2O}

The MABRs were operated simulating a retrofit with MABR in the anaerobic bio-p zone of Ejby Mølle WRRF, in which MABRs would carry out substantial N removal, followed by an activated sludge, which, under considerably lower nitrogen loading rates (NLR), would carry out the remaining treatment to reach effluent discharge limits. Therefore, the MABRs were operated at a high $NH_{x,load}$, and relatively low % NH_x removal (compared with a complete BNR system) (Table 2).

Table 2. Summary of nitrogen removal performance and N_2O emissions. Annual daily values (first row) and corresponding coefficient of variation (second row). Daily coefficients of variation (third row)

		$NH_{x,load}$	**ΔNH_x**	**OTR**	**NTR_{exh}**	**NTR_{bulk}**	**$NTR_{bulk,aer}$**	**$NTR_{bulk,un}$**	**EF_{N2O}**
		kg N d^{-1}	g N d^{-1}	kg O_2 d^{-1}	g N d^{-1}	g N d^{-1}	g N d^{-1}	g N d^{-1}	% N load
R1	Annual	**5.90±3.01**	**1852±894**	**18.3±3.7**	**38±21**	**15±32**	**23±41**	**6±9**	**0.88±1.28**
	Seasonal variability	51%	48%	20%	56%	213%	178%	163%	146%
	Diurnal variability	19±14 %	37±26%	7±4	26±24%	136±301%	120±157%	107±321%	42±43%
R2	Annual	**4.19±2.03**	**1104±556**	**12.6±7.1**	**24±23**	**16±32**	**37±65**	**3**±4	**0.82±0.86**
	Seasonal variability	49%	50%	57%	94%	194%	174%	149%	105%
	Diurnal variability	19±14%	33±18%	12±10	41±27%	233±435%	136±226%	193±398%	75±48%

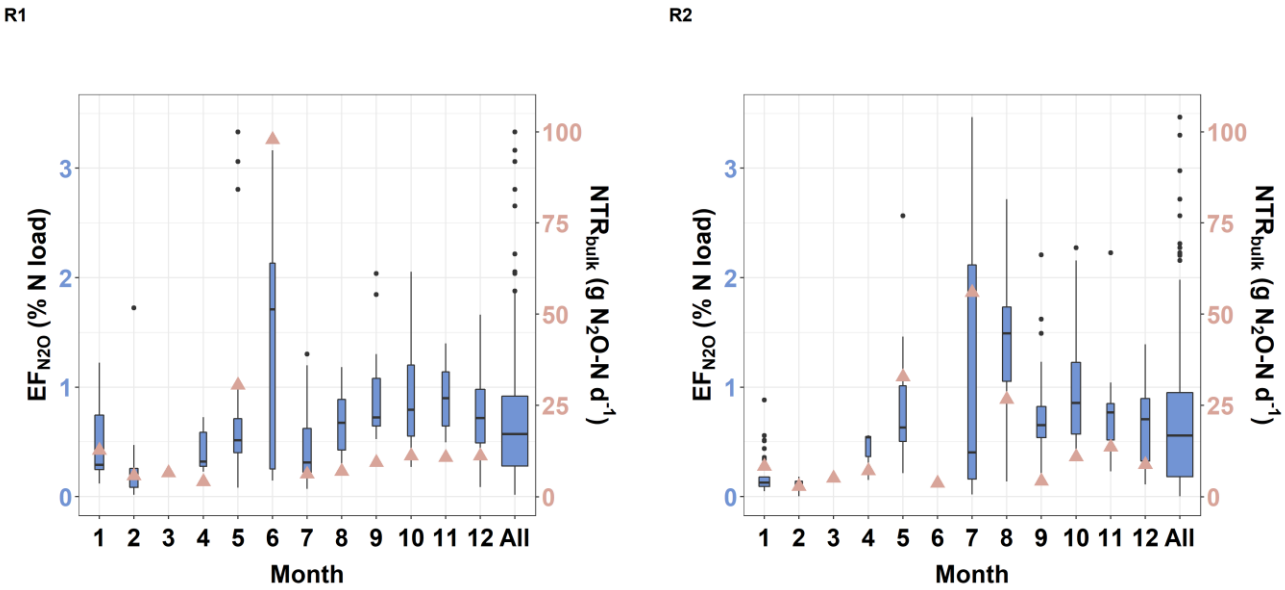

228

229 **Fig 2.** N_2O emission factors in R1 and R2 per month, average N_2O transfer rates from the bulk per
230 month.
231

232 The average EF_{N2O} was 0.88±1.28 and 0.82±0.86 % (Table 2), and the median values were 0.51 and
233 0.48%, respectively (Fig 2). The highest EF_{N2O} values correspond to June in R1 and August in R2, which
234 include episodes with high NTR_{bulk} values.

235 The largest spreads in the dataset can be seen in NTR_{bulk}, both in $NTR_{bulk,aer,}$ and $NTR_{bulk,un}$, in all three
236 aspects more than in NTR_{exh} (Table 2): seasonal variation, which indicates significant differences
237 between months and seasons, diurnal variation average, which is an indication of a highly dynamic
238 system, and the diurnal standard deviation, which highlights significant differences between days.
239 Overall, the EF_{N2O} results show large seasonal variabilities (146% and 105%) but moderate diurnal
240 variabilities (42±43% and 75±48%). The OTR shows the lowest seasonal and diurnal variabilities, and
241 both $NH_{x,load}$ and NH_x removal also show low seasonal and diurnal variabilities, generally lower than
242 50% (Table 2).

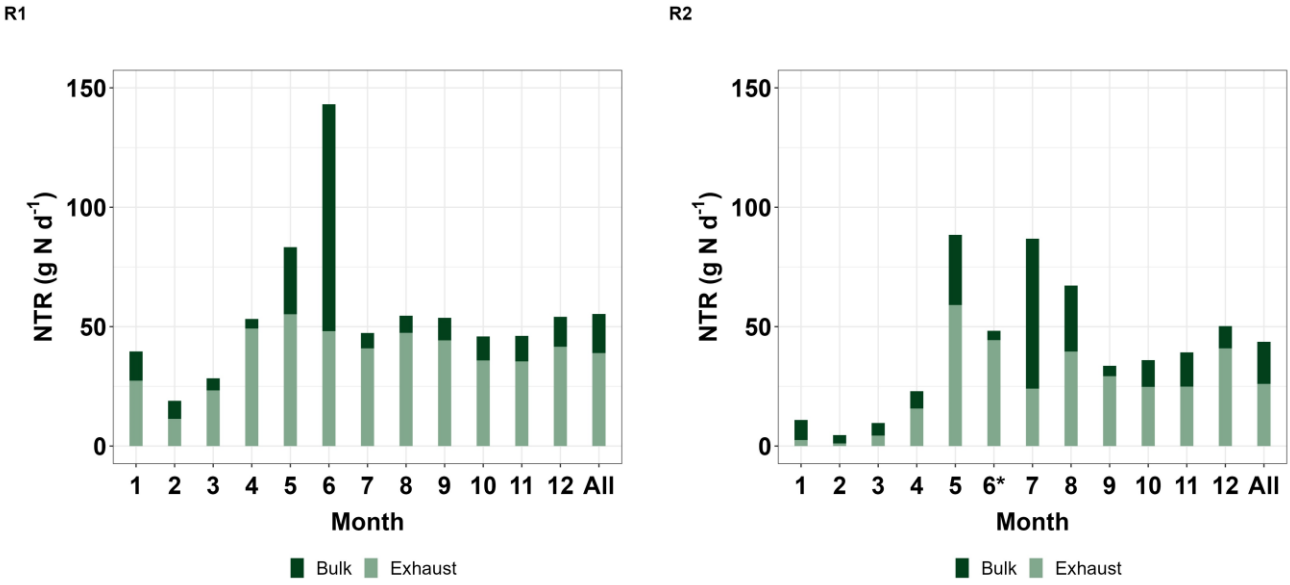

Fig 3. Average N_2O transfer rates from R1 and R2 per month. Dark green for emissions from the bulk and light green for emissions from the MABR exhaust. (*Only 4 days of data in R2 month 6)

N_2O was emitted predominantly through the MABR exhaust, with NTRs typically below 50 g N d^{-1} (Fig 3). There was an increase in NTR_{bulk} values in R1 during May and June, with the latter being the month with the highest emissions from the study (almost 150 g N_2O-N d^{-1}). In R2, NTR_{bulk} also increased during the warmer months: May, July and August.

Although the contributions from NTR_{bulk} to the total NTR appear to be very significant (Table 2), 30 and 60% of the NTR total (Table 2), NTR_{bulk} is only a small percentage of the total during most months (Fig. 3). The daily average data distributions are positively skewed (Fig S1), where extreme events with very high NTR_{bulk} significantly increase the monthly and annual average, which coincides with the observations from Fig 3 and Table 2.

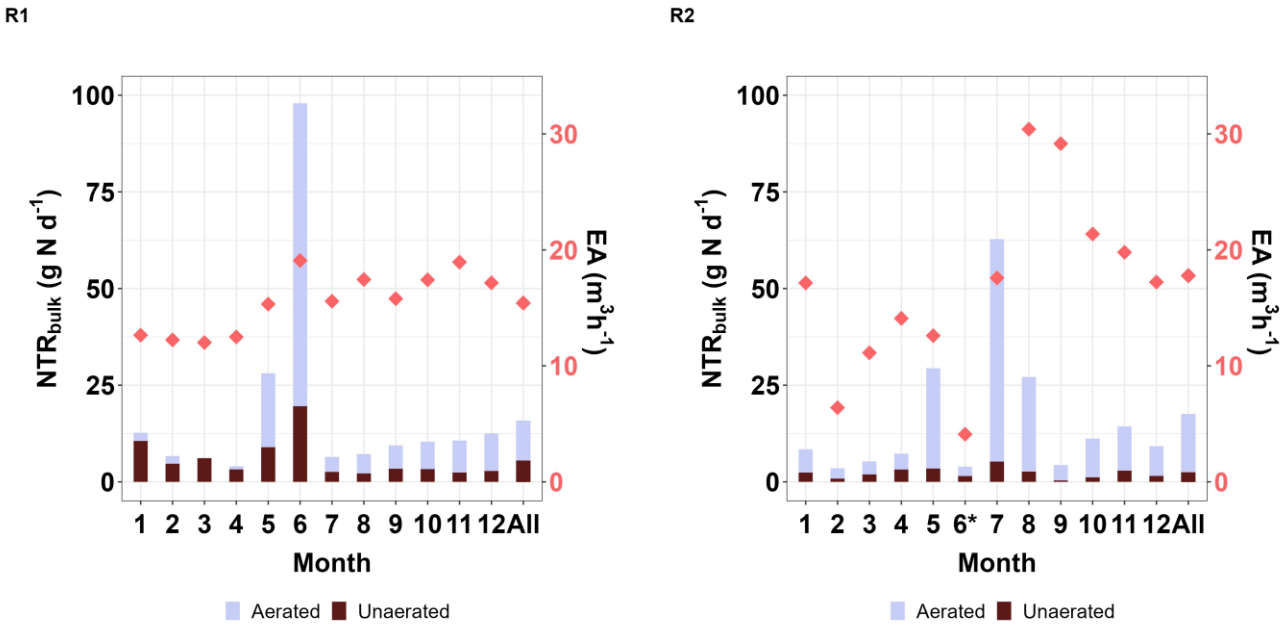

Fig 4. Average N_2O transfer rates from R1 and R2 per month. Dark purple for emissions from the bulk during non-aerated periods (EA off) and light purple for emissions from the bulk during aerated periods (EA on). Average EA use per month as pink points. (*Only four days of data in R2 month 6)

As described in section 2.3.2, for both R1 and R2, the mass transfer coefficient (K_La) used to calculate NTR_{bulk} (Eq. 4b) varies substantially depending on whether the bulk mixed liquor was aerated with EA or not. $NTR_{bulk,aer}$ was on average much higher than $NTR_{bulk,un}$ (Fig 4). Results reveal that high NTR_{bulk} resulted from external aeration and, therefore, high $NTR_{bulk,aer}$, and were the highest during June in R1 / July in R2.

3.2 MULTIVARIATE ANALYSIS OF EMISSIONS

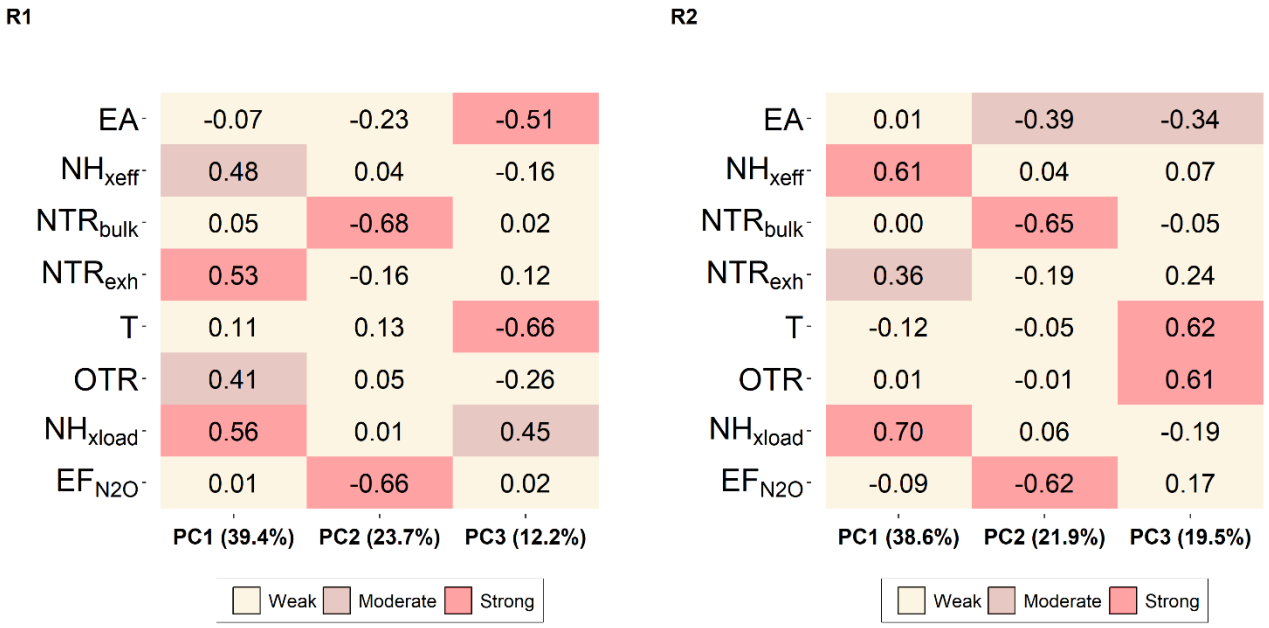

Fig 5. Loadings from principal component analysis of R1 and R2 after Promax rotation. Loadings are considered: weak (<0.3), moderate (<0.5) and strong (>0.5).

One-minute frequency observations (n ≈ 300.000) from both R1 and R2 were mined using PCA. During analysis, variables which did not significantly contribute to the model were discarded, and the dataset (containing both observed and calculated variables) was reduced from approximately 20 variables to 8. The three first PCs were able to explain 75 and 78% of the variability in the data for R1 and R2, respectively. The variables had similar loadings and correlations in both reactors, with minor differences (Fig 5). For R1, PC1 (which explains 39.4% of the variability) shows strong and positive correlations between NTR_{exh} and $NH_{x,load}$ and moderate correlations between $NH_{x,eff}$, and OTR. Similarly, PC1 for R2 (36.8% variability) shows strong and positive correlations for NTR_{exh}, $NH_{x,load}$, and moderate

correlations for $NH_{x,eff}$ (but not OTR). This clearly indicates that at higher $NH_{x,load}$, more emissions from the exhaust MABR gas can be expected.

For PC2, which explains 23.7 and 21.9% of the variability in R1 and R2 respectively, we find a strong (positive) correlation between EF_{N2O} and the NTR_{bulk}, and a moderate correlation with EA but only in R2. This shows that the emission fraction from the bulk mixed liquor significantly impacts the final overall EF_{N2O}, and confirms that this is related to the use of EA.

In the third PC, which explains 12.2 and 19.5% of the variability, we find the most significant dissimilarities between the two reactors. In R1, EA and temperature are strongly positively correlated, and there is a moderate contribution from $NH_{x,load}$ in the opposite direction. In contrast, in R2 we find strong (positive) correlations between OTR and temperature and a moderate correlation to EA in the opposite direction. It is essential to highlight that the ORP-based control strategy (see section 2.1.2) manipulated both $NH_{x,load}$ and EA, and had to be adjusted differently throughout the study period in R1 and R2. ORP-control is therefore likely responsible for the inconsistencies in PC3.

The results from an alternative PCA using daily average values, including only samples when laboratory analysis for nitrite, nitrate and COD were available, can be seen in Fig S2 (n = 47). Results show similarities in the relationship between EA and NTR_{bulk} and $NH_{x,load}$ and NTR_{bulk} and NTR_{ex} compared to the PCA analysis in Fig 5. Moderate or strong correlations including the new variables (nitrite, nitrate and C/N ratio) were present only in PC3 (14/16% variability) and PC4 (9/9% variability) Nitrite and nitrate show a strong correlation to each other and a moderate positive correlation to the C/N ratio (exclusively in R1). The CN ratio was further moderately correlated to NTR_{exh} and NTR_{load} in R1 and to EA in R2.

3.3 N_2O DYNAMICS AND DIURNAL PATTERNS

Fig 6 shows an example of a typical diurnal pattern during the study, where $NH_{x,load,}$ and $NH_{x,eff}$ present a similar daily trend profile (R-A,B). At the same time, N_2O gaseous concentrations in the exhaust (R-D) follow the pattern of the $NH_{x,load}$ and $NH_{x,eff}$. N_2O concentrations in the bulk, (R- C), appear to have a baseline value below 0.05 g N m^{-3}, and peaks that do not correspond to changes in $NH_{x,load}$ or $NH_{x,eff}$ (R-A,B). Interestingly, these disturbances or peaks coincide in both the bulk and exhaust and can be attributed to the effect of coarse bubble aeration used for biofilm scouring.

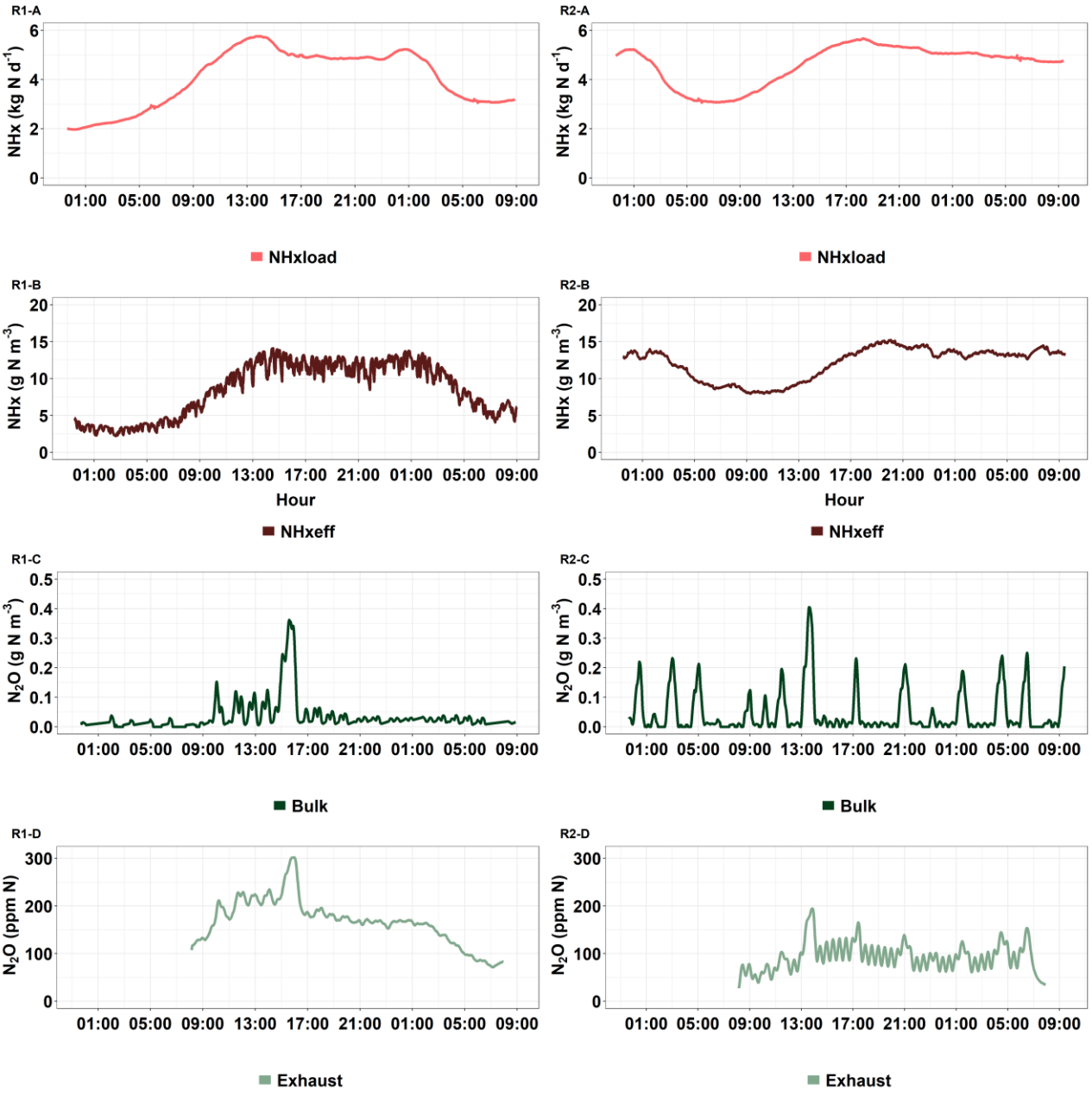

Fig 6. $NH_{x,load}$ (A) and $NH_{x,eff}$ (B) and N_2O concentration in the bulk (C) and in the MABR exhaust (D) during 36h in R1 (13-14th) and R2 (14th-15th) in November 2020

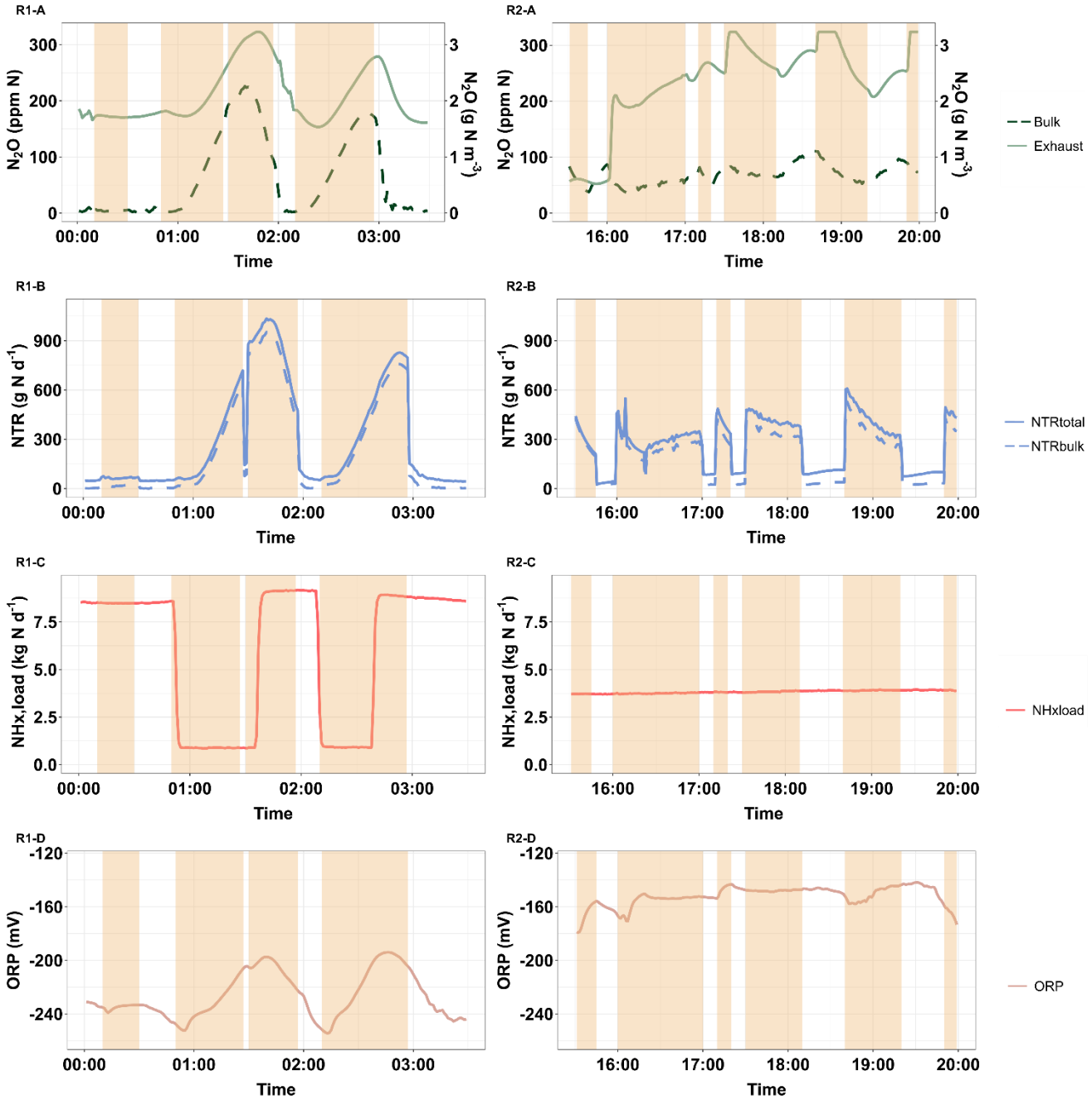

Fig 7. Profiles for R1 and R2 showing N_2O concentrations in the bulk (A – right axis) and the MABR exhaust (A- left axis), N_2O transfer rates (B – solid line) and the contribution from bulk emissions only (B- dashed line), ammonia/um load (C) and ORP level in the reactor (D). Shadowed area in light yellow represents periods of time when EA was on. 12th July 2020 in R1 and 14th October 2020 in R2.

Fig 7 shows an example from R1 (left) and R2 (right) during an episode of high NTR_{bulk} emissions events to better understand the dynamics in place. The ORP control strategy, which was triggered especially during the warmer summer months, significantly affected the NTR total. This is mainly due to the manipulation of both the use of EA and $NH_{x,load}$ control (see section 2.2.2).

In the example from R1, N_2O production in the bulk surpasses stripping rates, as N_2O accumulates during aerated periods (Fig 7 R1-A). On the other hand, the example for R2 shows a situation where N_2O production is lower than stripping rates, and N_2O accumulates in the bulk during unaerated periods, and it is stripped during aerated periods (Fig 7 R2-A).

At moderate and stable ORP values of approximately -160 mV (Fig 7 R2-D) the $NH_{x,load}$ control was not triggered (Fig 7 R2-C) and resulted in NTR total values in between 300 and 600 g N d^{-1} (Fig 7 R2-B). However, we can see in the example from R1, that when $NH_{x,load}$ was reduced due to low ORP values (< -250 mV, approx. time 1 am) (Fig 7 R1-C, D) this resulted in much higher NTR total values of close to 1000 g N d^{-1}(Fig 7 R1-B).

A combination of low feed and aerated bulk conditions increased N_2O dissolved concentrations to values close to 2 g N m^{-3} (Fig 7 R1-A, 1-3 am). When the feed was turned up again (R1-C) before 2 am, even though the EA was still on, the concentration of N_2O started to decline (Fig 7 R1-A). The concentration of N_2O in the MABR exhaust followed the bulk concentration (with a lag) in R1-A, which seems to indicate that at such high dissolved concentrations, a flux of N_2O is driven from the bulk into the biofilm, and into the membrane lumen. Moreover, an aerobic layer possibly develops in the outer part of the biofilm, preventing any biological N_2O reduction.

3.4 EMISSION FACTORS: VARIABILITY AND SCENARIO ANALYSIS

Scenario one (SC1), shows the average annual EF_{N2O} was 0.86±1.11 % (Fig 8, Table S1), almost half of the standard IPCC 2019 value of 1.6%, and very similar to the later published national emission factor for Denmark of 0.84% (Vangsgård and Madsen, 2020) and for Switzerland 0.9 % (Vogt et al., 2021). As was seen in Table 2, the large standard deviation can be attributed to seasonal variations and the impact of the large variability in the NTR_{bulk} data.

Scenario two (SC2) equals SC1 with the addition of the N_2O emissions from bulk liquid discharged with the effluent. This fraction should be accounted for if no downstream processes can result in either stripping or reduction of N_2O. In this study, the MABRs discharged into a 1000 m^3 bio-p anaerobic zone, and it is reasonable to assume that the small quantity of N_2O dissolved in the MABR effluent will be reduced in this tank. However, if this were not the case, the $EF_{N2O,}$ including liquid emission, would increase to 1.33±1.64 % (Fig 8).

Scenario three (SC3) and scenario four (SC4) correspond to $EF_{N2O,ANH,}$ and $EF_{N2O,OTR}$, which is another method to report EF_{N2O} based on NH_x removal instead of loading. Since the MABRs did not carry out a significant fraction of NH_x removal, SC3 and SC4 emissions are more considerable than SC1, 5.47±6.80%, and 1.32±1.24±%, respectively. It is worth noting how calculating NR based on OTR dramatically reduces both the average value and the variability (Fig 8).

Scenarios five (SC5) and six (SC6) refer to alternative ways to calculate and report the EF_{N2O} from SC1. SC5 only considers EF_{N2O} estimations when laboratory analysis data is available. Unless enough data points are accounted for, performance dynamics and extreme events might be left out, thus reducing data variability, which did not change in this study for 72 data points (0.89±0.83) (Fig 8). SC6 considers how

much impact extreme NTR_{bulk} values have. The top 10% of NTR values was removed from the dataset (90^{th} percentile), which is likely to occur in short-term monitoring campaigns. This resulted in an EF_{N2O} value that was 33% lower than SC1 (0.58±0.4%).

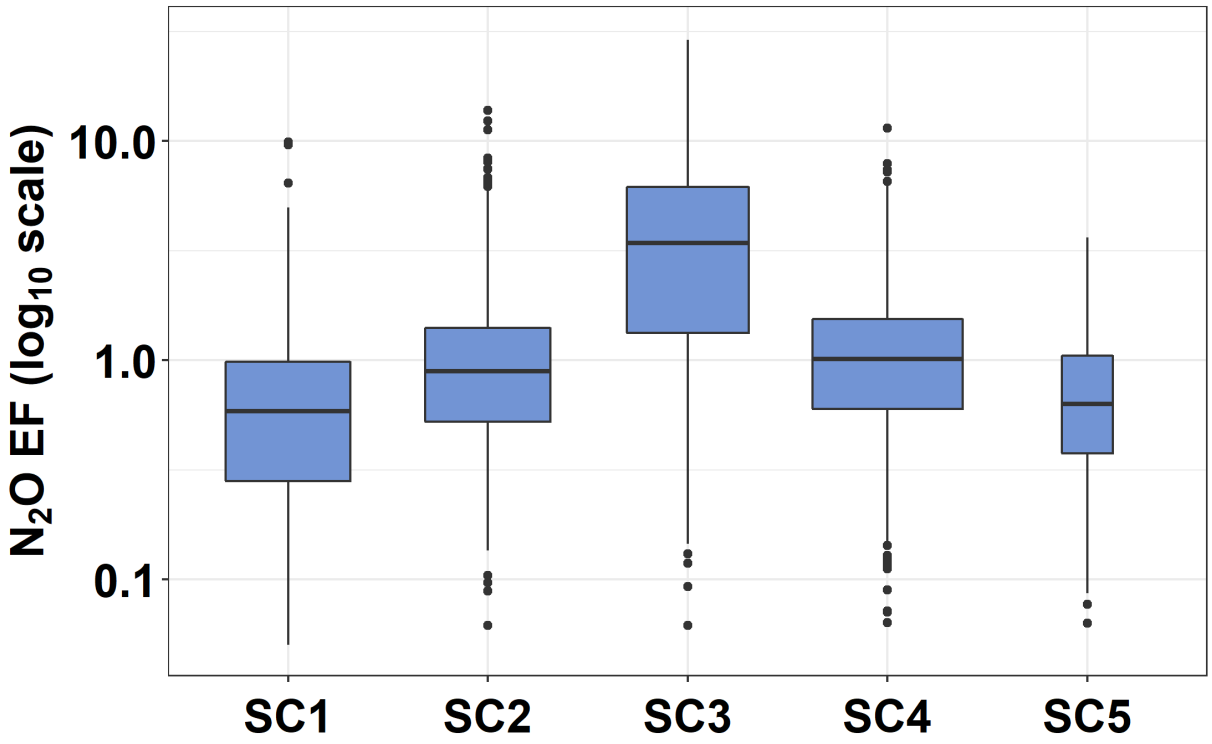

Fig 8. N_2O emission factors calculated using five different methods using average daily data. Logarithmic scale in y-axis..

4 DISCUSSION

4.1 REPORTING OF EMISSION FACTORS

To assess and reduce the environmental impact of advanced N removal processes, the accurate quantification of EF_{N2O} is essential. The current methods for estimating EF_{N2O} are oversimplified, unreliable, and not representative of different process configurations or conditions (Adam and Van Briesen, 2017), and benchmarking and comparability are challenging due to the inconsistencies in the reported data available (Massara et al., 2017; Vasilaki et al., 2019).

The duration of the monitoring campaign is critical. Vasilaki et al., 2019 analyzed more than 70 full-scale campaigns and found those that lasted less than one month obtained EF_{N2O} values lower than 0.3%, while long-term campaigns over a year-long resulted in much higher values (1.7% median). Monitoring campaigns that are too short to capture extreme events and seasonal trends will likely underestimate emission factors. In this study, high-emission events in the bulk significantly affect the overall EF (Table 2) and the top 10% of the data set is responsible for increasing the annual average EF_{N2O} from 0.58 to 0.86% (Fig 8). If monthly averages are used instead of daily averages, this will also lead to a miscalculation of the importance of extreme events.

EF_{N2O} had a high seasonal variability (Table 2) and the highest emissions occurred during the warmest months of the year (see Fig 2,3,4). At least one study has also found emissions to increase also concurrent to temperature increase (Daelman et al., 2015), while this effect was not observed in other studies (Kosonen et al., 2016; Gruber et al., 2020). This inconsistency could be explained by the fact that in some cases, at higher temperatures higher $NH_{x,load}$ occurs, and therefore temperature could act as a $NH_{x,load}$

388 proxy. Indeed, in this study the multivariate analysis showed NTR was not correlated to temperature but
389 to $NH_{x,load}$ instead (Fig 2), as did Kosonen et al., 2016 and Gruber et al., 2020.

390 The frequency of the data acquisition is also essential to EF_{N2O} reporting. Daelman et al., 2013 used a
391 long-term data set with continuous N_2O data from a full-scale installation and indicated that short
392 sampling campaigns (single grab samples, 24h or seven days), did not estimate the average EF_{N2O}
393 adequately close to the true average. Moreover, infrequent $NH_{x,load}$ analysis could lead to added
394 uncertainty in EFs even when using continuous N_2O data. However, in this study, we found that
395 continuous online data and daily averages when laboratory samples were available resulted in an almost
396 identical annual average EF_{N2O} (see Fig 8). This could be attributed to the high number of samples for
397 $NH_{x,load}$ (n = 72), which is much higher than it is typical for full-scale facilities (n =12 per year). Even
398 if overall EF_{N2O} values are similar, only online monitoring can capture diurnal trends and correlations to
399 operational variables. In this study, we found N_2O emissions followed a diurnal trend which could be
400 traced back to the diurnal NH_x loading rate (Fig 6, 7). Similar findings are also reported in Daelman et
401 al., 2015 and Valkova et al., 2021.

402 Lastly, EF_{N2O} values are sometimes reported in terms of % NH_x removed, not $TN_{,load}$, especially in partial
403 nitritation/anammox (PN/A) (Joss et al., 2009; Pijuan et al., 2014; Yan et al., 2014; Bellandi et al., 2017),
404 which can be troublesome when comparing different nitrogen removing technologies. In this study, we
405 show EF_{N2O} based on NH_x removal calculated using OTR and NH_x measurements and how this resulted
406 in increased EF_{N2O}, especially when using NH_x sensor data, which has almost double the diurnal
407 coefficient of variability than $NH_{x,\ load}$ (see Fig 8, Table 2) and three to five times larger than OTR.
408 Moreover, using OTR to calculate NH_x removal in MABRs can lead to overestimating removal rates
409 and, therefore, an underestimation of EF_{N2O}.

In conclusion, our results highlight the impact of different methods to calculate EF_{N2O} and how not including the effluent liquid fraction, seasonal and extreme events (with sufficiently frequent data acquisition and duration of the monitoring campaign) would lead to underestimating $EF_{N2O.}$ Finally, due to the inherent variability in the data (diurnal and seasonal), not only average annual values but also standard deviations should be used to compare and diagnose EF_{N2O} results.

4.2 BENCHMARK

A strong and significant correlation (R^2 = 0.65, p-value < 0.001) was found between the NLR to a treatment process reactor (g N load per m^3 reactor volume per d) and the EF_{N2O} from screening reported data (Fig 9). Exclusively data from full-scale installations, during long-term campaigns collecting high-frequency data was considered. When the MABR results from this study were not included, R^2 increased to 0.73 (p-value < 0.001), indicating our results do not follow the general trend. More details on the data used to build the graph can be found in Table S2.

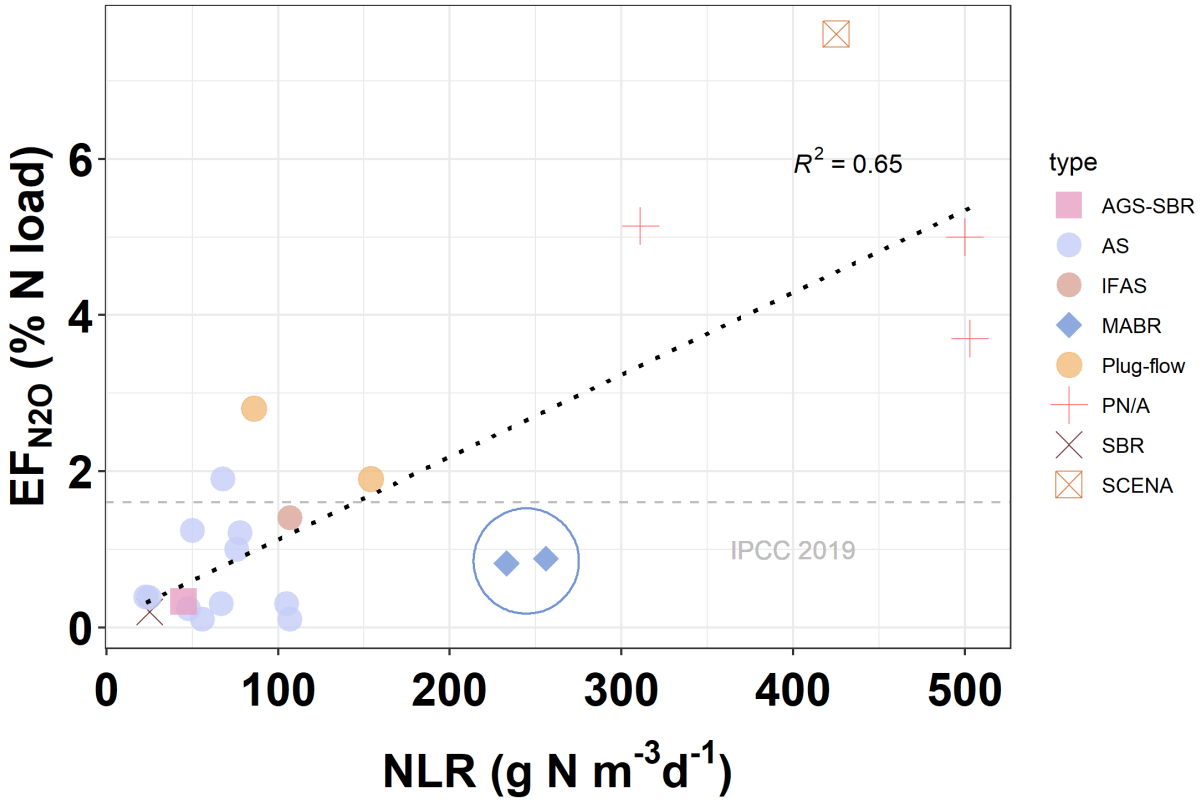

Fig 9. Benchmark of different types of biological N removal technologies according to the % of N load emitted as N_2O-N (y-axis) and the nitrogen loading rate (g N m^{-3} d^{-1}) (x-axis).

In addition, the correlation presented in Fig 9 could help benchmark technologies based on N_2O emissions. Benchmarking EF_{N2O} for different NH_x-removal technologies is of utmost importance if water utilities are to consider this parameter when making decisions. Hence, those who fall above the trend line would have a lower score (higher than "expected" N_2O emissions) than those who fall below the trend line (lower than "expected" N_2O emissions).

This relationship between higher NLR and higher EF_{N2O} can be explained by the fact that at higher volumetric specific loading, higher NH_x turnover or ammonia oxidation rate (AOR) is expected, increasing production by NN, DN, and AP pathways (Blum et al., 2018). This has been pinpointed as one of the leading causes why PN/A technologies (right hand side of Fig 9) treating high strength reject water have, in general, higher EF_{N2O} values (Ribera-guardia and Pijuan, 2017).

A step-feed plug-flow treatment plant in Australia observed significantly more EF_{N2O} in the second step (3.5%) than in the first step (0.68%) (Fig 9). The second step received 50% of the influent, plus all the effluent N from step 1, and therefore, a higher specific N load is expected. The Ejby Mølle WRRF was monitored for six months in 2019, and three months into the campaign, the two reactors being monitored changed operation from parallel to series, resulting in a dramatic increase in N_2O emissions in the carrousel tank that was receiving double the specific N load after the change (Miljøstyrelsen, 2020).

We are aware that this approach is a simplification, as N_2O production and emissions are complex and affected by multiple variables, and different operational conditions and strategies can impact emissions (Vasilaki et al., 2018; Chen et al., 2020). Indeed, attempts to mitigate N_2O emissions from PN/A reactors have resulted in EF_{N2O} values lower than 1.6% (Weissenbacher et al., 2010; Uri-Carreño et al., 2017). It also explains the variability in emissions within plants with similar specific N loading (left hand side of Fig 9).

Results from this study, where R1 and R2 had average annual EF_{N2O} values of 0.88 and 0.82 % and NLR of 256 and 233 g N m^{-3} d^{-1}, would place MABR below the predicted EF_{N2O} (based on the linear model presented in Fig 9) of 2.67 and 2.39%. Although full-size, R1 and R2 were not equivalent to a complete BNR since the % NH_x removal was low (Table 2). The operating NH_x concentrations are consequently

higher, which means R1 and R2 operated at a high AOR, which increases N_2O production (Blum et al., 2018). A hybrid MABR removing a higher fraction of N would potentially have an even lower EF_{N2O}.

The top 10% of the NTR was responsible for an increase in the annual EF_{N2O} from 0.58 to 0.86% (Fig 8). And it was disturbances caused by the EA as part of an ORP control in the mixed liquor which caused high-emission episodes in the NTR_{bulk}, especially during the warmer months (Fig 2,3,5,7). Hence, future studies in hybrid MABRs, where the bulk remains anoxic could result in lower N_2O production than observed in this study.

We can conclude that the environmental conditions of the mixed liquor in which hybrid MABRs are placed will play a major role in the total NTR. Ideally, MABR should be located in anoxic reactors with sufficient carbon to achieve complete denitrification of any N_2O that could diffuse from the biofilm and prevent incomplete denitrification of other NO_x species resulting in N_2O accumulation. To reduce the production of N_2O in the MABR exhaust, linked to high NH_x turnover, alternative MABR aeration strategies could be implemented. For example, (Ma et al., 2021) demonstrated in a laboratory-scale MABR fed with NH_x and no external carbon that an intermittent aeration strategy achieved N removal and low N_2O emissions (EF_{N2O} 0.4%).

4.3 MECHANISMS OF N_2O PRODUCTION IN FULL-SCALE MABR

Scientific literature reports three main N_2O biological production pathways and one abiotic one (Schreiber et al., 2012; Domingo-Félez and Smets, 2016). Two of the biological processes are related to ammonia-oxidizing organisms (AOO) activity: the nitrifier-nitrification (NN) and nitrifier-denitrification (ND) pathway, while the third biological production pathway, heterotrophic denitrification (HD), is

related to ordinary heterotrophic organisms (OHO). The last pathway, abiotic production (AP), is related to the two chemical reactions driven by hydroxylamine (Heil et al., 2014).

Multivariate analysis revealed that NTR_{exh} was generally responsible for most of the emissions from the MABRs, except for the sporadic events with high NTR_{bulk} (see Fig 2, 3, 5). The exhaust emissions were mainly correlated to $NH_{x,load}$ and $NH_{x,eff}$ (see Fig 5), and showed similar diurnal variability (Table 2), indicating N_2O production was linked to one or more of the NH_x-oxidation-related pathways: NN, DN. This is consistent with the general knowledge that N_2O production in nitrifying biofilms is likely dominated by AOO activity (Sabba et al., 2018). Previous studies have shown that nitrifiers grow closer to the membrane lumen in MABRs (Terada et al., 2003), and N_2O production occurs primarily close to the biofilm-membrane interface (Kinh et al., 2017a). Liu et al., 2022 showed in a modeling study of an MABR performing simultaneous nitrification-denitrification that most of the N_2O turnover was regulated by the hydroxylamine-oxidation pathway. However, nitrite-oxidizing bacteria could also contribute to the emissions by consuming oxygen in the nitrifying zone of the biofilm and promoting oxygen-limited conditions (Sabba et al., 2016). The produced N_2O back diffuses into the membrane lumen, given that the membranes are operated open-ended with a constant air flux with atmospheric concentrations of N_2O.

NTR_{bulk} were further divided into emissions corresponding to 1) periods with EA ($NTR_{bulk,aer}$) and 2) periods without external aeration ($NTR_{bulk,un}$). Most months $NTR_{bulk,aer}$ values were close to or below the lower detection limit of 5.5 g N_2O-N d^{-1}. During these situations, the bulk remains anoxic, and any N_2O produced within the biofilm will diffuse back to the lumen. OHO could reduce it in either the anoxic outer layer of the biofilm (Kinh et al., 2017a) or in the mixed liquor (Conthe et al., 2019) containing readily biodegradable carbon from the feed. Therefore, N_2O emissions from the bulk during unaerated periods are either diffused from the biofilm or produced via the HD pathway.

The use of EA by the ORP control promoted the stripping and production of N_2O in the bulk (see Fig 7) and was responsible for an overall larger annual EF_{N2O} (Fig 2,3,5). The EA is not intended to be sufficient to support significant nitrification in the mixed liquor, as was previously confirmed (Uri-Carreño et al., 2021). The most likely mechanism driving N_2O production during episodes with EA is HD since even microaerobic conditions inhibit denitrification, and N_2O reduction is the most oxygen-sensitive step. As observed, a combination of EA and stopping the feed (no carbon available for denitrification) caused the highest NTR_{bulk} emissions episodes (Fig 7). HD has been shown to be the main N_2O production pathway using N-species isotope ratio measurements under anoxic conditions due to organic substrate limitation (Gruber et al., 2022).

We conclude that the most likely mechanisms for N_2O production were those related to nitrification activity in the MABR biofilm, and denitrification activity in the bulk. Natural abundance isotopic measurements would elucidate the contribution of each production pathway. One question remains as to what the role of the scouring aeration is, as it impacted the bulk and exhaust N_2O concentrations (Fig. 6,7). Moreover, in commercial applications, MABR exhaust air is internally recycled for scouring (R1) or mixing (R2), allowing for a potential transfer from the exhaust to the bulk, and the implications on overall emissions should be further investigated.

CONCLUSIONS

The main findings of this article can be summarized in the following points:

- EF_{N2O} values from both MABRs (R1, R2) were similar in overall quantity and dynamics. N_2O was emitted predominantly from the MABR exhaust gas (NTR_{exh}) but sporadic high emissions

from the bulk ($NTR_{buk,aer}$) mixed liquor caused by the EA contributed largely to the annual average EF_{N2O}.

- NTR_{exh} follows the pattern of the $NH_{x,load}$ and concentration. In periods with low ORP values and $NH_{x,load}$, the actions taken by the implemented control system promoted an increased N_2O flux from the bulk into the biofilm and the membrane lumen.
- Process data suggest that $NTR_{exhaust}$ was linked to one or more of the NH_x-oxidation related pathways: NN and ND. While for NTR_{bulk}, HD seems to be the most likely pathway (during both externally aerated and unaerated periods).
- Different methods for calculating and reporting EF_{N2O} show the importance of including liquid emissions when relevant, long-term monitoring to include extreme events, and the added variability when using data from NH_x sensors versus laboratory analysis or calculations based on OTR.
- A strong and significant correlation ($R^2 = 0.65$, p-value < 0.001) was found between the NLR (N load in g N m^{-3} d^{-1}) and the % of the N load emitted as N_2O-N (EF_{N2O}). This allows to benchmark treatment technologies according to; 1) higher and 2) lower than "expected" N_2O emissions. The obtained EF of 0.88 and 0.82 % and NLR of 256 and 233 g N m^{-3} d^{-1}, would place MABR as a technology capable of achieving intensification at "lower than expected" N_2O emissions.
- Future studies should investigate the effects of mixing and scouring processes in MABRs on N_2O production and emission.

Acknowledgments

The authors would like to acknowledge the contributions of Kevan Brian and Isabel Telles Silveira for their insightful discussions on the topic of full-scale hybrid MABRs and N_2O emissions. Nerea Uri-

Carreño gratefully acknowledges the Industrial Ph.D. program's financial support from Innovation Fund Denmark, through the project "MANTRA" (Contract-No: 7091-00038A). Dr. Xavier Flores-Alsina and Prof. Krist Gernaey also thank, the Danida fellowship center (DFC) research project ERASE (Contract-No: 18-M09-DTU). Dr. Carlos Domingo-Félez thanks the Fermentation-based Biomanufacturing Initiative (FBM), grant number NNF17SA0031362. All authors received the financial support of the Miljøministeriets Miljøteknologisk Udviklings og Demonstrationsprogram (MUDP) project NACAT (Contact-No: 2021-20015)

Software availability

Processed data and statistical tools used to conduct this study are available on request. To express an interest in these, contact Nerea Uri-Carreño at Vand Center Syd (nur@vandcenter.dk)

5 REFERENCES

Adam, C., Van Briesen, J.M., 2017. Incorporating Uncertainty into Future Estimates of Nitrous Oxide Emissions from Wastewater Treatment. J. Environ. Eng. 143, 4017029. https://doi.org/10.1061/(ASCE)EE.1943-7870.0001231

G. Aydin (2014) The Modeling of Coal-related CO2 Emissions and Projections into Future Planning, Energy Sources, Part A: Recovery, Utilization, and Environmental Effects, 36:2, 191-201, DOI: 10.1080/15567036.2012.760018

Bellandi, G., Porro, J., Senesi, E., Caretti, C., Caffaz, S., Weijers, S., Nopens, I., Gori, R., 2017. Multi-point monitoring of nitrous oxide emissions in three full-scale conventional activated sludge tanks in Europe. Water Sci. Technol. 77, 880–890. https://doi.org/10.2166/wst.2017.560

Blum, J.-M., Jensen, M.M., Smets, B.F., 2018. Nitrous oxide production in intermittently aerated Partial Nitritation-Anammox reactor: oxic N2O production dominates and relates with ammonia removal rate. Chem. Eng. J. 335, 458–466. https://doi.org/https://doi.org/10.1016/j.cej.2017.10.146

Carlson, A.L., He, H., Yang, C., Daigger, G.T., 2021. Comparison of hybrid membrane aerated biofilm reactor (MABR)/suspended growth and conventional biological nutrient removal processes. Water Sci. Technol. 83, 1418–1428. https://doi.org/10.2166/wst.2021.062

Castrillo, M., Díez-Montero, R., Esteban-García, A.L., Tejero, I., 2019. Mass transfer enhancement and improved nitrification in MABR through specific membrane configuration. Water Res. 152, 1–11. https://doi.org/10.1016/j.watres.2019.01.001

Chen, H., Zeng, L., Wang, D., Zhou, Y., Yang, X., 2020. Recent advances in nitrous oxide production and mitigation in wastewater treatment. Water Res. 184, 116168. https://doi.org/https://doi.org/10.1016/j.watres.2020.116168

Conthe, M., Lycus, P., Arntzen, M., Ramos da Silva, A., Frostegård, Å., Bakken, L.R., Kleerebezem, R., van Loosdrecht, M.C.M., 2019. Denitrification as an N2O sink. Water Res. 151, 381–387. https://doi.org/10.1016/j.watres.2018.11.087

Daelman, M.R.J., De Baets, B., van Loosdrecht, M.C.M., Volcke, E.I.P., 2013. Influence of sampling strategies on the estimated nitrous oxide emission from wastewater treatment plants. Water Res. 47, 3120–3130. https://doi.org/10.1016/j.watres.2013.03.016

Daelman, M.R.J., van Voorthuizen, E.M., van Dongen, U.G.J.M., Volcke, E.I.P., van Loosdrecht, M.C.M., 2015. Seasonal and diurnal variability of N2O emissions from a full-scale municipal wastewater treatment plant. Sci. Total Environ. 536, 1–11.

https://doi.org/10.1016/j.scitotenv.2015.06.122

Danish Government, 2020. Aftale mellem regeringen (Socialdemokratiet) og Venstre, Radikale Venstre, Socialistisk Folkeparti, Enhedslisten, Det Konservative Folkeparti, Liberal Alliance og Alternativet om Klimaplan for en grøn affaldssektor. Klimaplan en grøn affaldssektor og cirkulær økonomi 1–17.

de Haas, D., Andrews, J., 2022. Nitrous oxide emissions from wastewater treatment - Revisiting the IPCC 2019 refinement guidelines. Environ. Challenges 8, 100557. https://doi.org/10.1016/j.envc.2022.100557

Delre, A., ten Hoeve, M., Scheutz, C., 2019. Site-specific carbon footprints of Scandinavian wastewater treatment plants, using the life cycle assessment approach. J. Clean. Prod. 211, 1001–1014. https://doi.org/https://doi.org/10.1016/j.jclepro.2018.11.200

Domingo-Félez, C., Smets, B.F., 2016. A consilience model to describe N2O production during biological N removal. Environ. Sci. Water Res. Technol. 2, 923–930. https://doi.org/10.1039/C6EW00179C

Downing, L.S., Nerenberg, R., 2008. Total nitrogen removal in a hybrid, membrane-aerated activated sludge process. Water Res. 42, 3697–3708. https://doi.org/10.1016/j.watres.2008.06.006

Faragò, M., Damgaard, A., Madsen, J.A., Andersen, J.K., Thornberg, D., Andersen, M.H., Rygaard, M., 2021. From wastewater treatment to water resource recovery: Environmental and economic impacts of full-scale implementation. Water Res. 204. https://doi.org/10.1016/j.watres.2021.117554

Gruber, W., Villez, K., Kipf, M., Wunderlin, P., Siegrist, H., Vogt, L., Joss, A., 2020. N2O emission in full-scale wastewater treatment: Proposing a refined monitoring strategy. Sci. Total Environ. 699,

134157. https://doi.org/https://doi.org/10.1016/j.scitotenv.2019.134157

Gruber, W., Magyar, P. M., Mitrovic, I., Zeyer, K., Vogel, M., von Känel, L., Biolley, L., Werner, R. A., Morgenroth, E., Lehmann, M. F., Braun, D., Joss, A., & Mohn, J. (2022). Tracing N2O formation in full-scale wastewater treatment with natural abundance isotopes indicates control by organic substrate and process settings. Water research X, 15, 100130. https://doi.org/10.1016/j.wroa.2022.100130

He, H., Wagner, B.M., Carlson, A.L., Yang, C., Daigger, G.T., 2021. Recent progress using membrane aerated biofilm reactors for wastewater treatment. Water Sci. Technol. 00, 1–27. https://doi.org/10.2166/wst.2021.443

Heil, J., Wolf, B., Brüggemann, N., Emmenegger, L., Tuzson, B., Vereecken, H., Mohn, J., 2014. Site-specific 15N isotopic signatures of abiotically produced N2O. Geochim. Cosmochim. Acta 139, 72–82. https://doi.org/https://doi.org/10.1016/j.gca.2014.04.037

Houweling, D., Daigger, G.T., 2019. Intensifying Activated Sludge Using Media-Supported Biofilms, 1st Editio. ed. CRC Press.

Irandoust, M. (2016). The renewable energy-growth nexus with carbon emissions and technological innovation: Evidence from the Nordic countries. Ecological Indicators, 69, 118–125. https://doi.org/10.1016/J.ECOLIND.2016.03.051

Jenni, S., Mohn, J., Emmenegger, L., Udert, K.M., 2012. Temperature dependence and interferences of NO and N2O microelectrodes used in wastewater treatment. Environ. Sci. Technol. 46, 2257–2266. https://doi.org/10.1021/es2032357

Joss, A., Salzgeber, D., Eugster, J., König, R., Rottermann, K., Burger, S., Fabijan, P., Leumann, S.,

Mohn, J., Siegrist, H.R., 2009. Full-scale nitrogen removal from digester liquid with partial nitritation and anammox in one SBR. Environ. Sci. Technol. 43, 5301–5306. https://doi.org/10.1021/es900107w

Kinh, C.T., Riya, S., Hosomi, M., Terada, A., 2017a. Identifi cation of hotspots for NO and N 2 O production and consumption in counter- and co-di ff usion bio fi lms for simultaneous nitri fi cation and denitri fi cation 245, 318–324. https://doi.org/10.1016/j.biortech.2017.08.051

Kinh, C.T., Suenaga, T., Hori, T., Riya, S., Hosomi, M., Smets, B.F., Terada, A., 2017b. Counter-diffusion biofilms have lower N2O emissions than co-diffusion biofilms during simultaneous nitrification and denitrification: Insights from depth-profile analysis. Water Res. 124, 363–371. https://doi.org/10.1016/j.watres.2017.07.058

Kosonen, H., Heinonen, M., Mikola, A., Haimi, H., Mulas, M., Corona, F., Vahala, R., 2016. Nitrous Oxide Production at a Fully Covered Wastewater Treatment Plant: Results of a Long-Term Online Monitoring Campaign. Environ. Sci. Technol. 50, 5547–5554. https://doi.org/10.1021/acs.est.5b04466

Kunetz, T.E., Oskouie, A., Poonsapaya, A., Peeters, J., Adams, N., Long, Z., Côté, P., 2016. Innovative membrane-aerated biofilm reactor pilot test to achieve low-energy nutrient removal at the Chicago MWRD. Weftec 2016 - 89th Water Environ. Fed. Annu. Tech. Exhib. Conf. https://doi.org/10.2175/193864716819713006

Liu, Yingrui, Zhu, T., Ren, S., Zhao, T., Chai, H., Xu, Y., Peng, L., Liu, Yiwen, 2022. Contribution of nitrification and denitrification to nitrous oxide turnovers in membrane-aerated biofilm reactors (MABR): A model-based evaluation. Sci. Total Environ. 806, 1–9.

https://doi.org/10.1016/j.scitotenv.2021.151321

Ma, Y., Piscedda, A., Veras, A.D.L.C., Domingo-Félez, C., Smets, B.F., 2021. Strategies of intermittent aeration to regulate microbial activities in membrane-aerated biofilm reactors: energy-efficient nitrogen removal and low nitrous oxide emission. Chem. Eng. J. 133630. https://doi.org/10.1016/j.cej.2021.133630

Massara, T.M., Malamis, S., Guisasola, A., Baeza, J.A., Noutsopoulos, C., Katsou, E., 2017. A review on nitrous oxide (N2O) emissions during biological nutrient removal from municipal wastewater and sludge reject water. Sci. Total Environ. 596–597, 106–123. https://doi.org/https://doi.org/10.1016/j.scitotenv.2017.03.191

Matter-Müller, C., Gujer, W., Giger, W., 1981. Transfer of volatile substances from water to the atmosphere. Water Res. 15, 1271–1279. https://doi.org/10.1016/0043-1354(81)90104-4

Miljøstyrelsen, 2020. MUDP Lattergaspulje Dataopsamling på måling og reduktion af lattergasemissioner fra renseanlæg.

Monje, V., Owsianiak, M., Junicke, H., Kjellberg, K., Gerneay, K., Flores-alsina, X., 2022. Economic, technical, and environmental evaluation of retrofitting scenarios in a full-scale industrial wastewater treatment system. Submitt. to Water Res.

Pellicer-Nàcher, C., Sun, S., Lackner, S., Terada, A., Schreiber, F., Zhou, Q., Smets, B.F., 2010. Sequential Aeration of Membrane-Aerated Biofilm Reactors for High-Rate Autotrophic Nitrogen Removal: Experimental Demonstration. Environ. Sci. Technol. 44, 7628–7634. https://doi.org/10.1021/es1013467

Pijuan, M., Torà, J., Rodríguez-Caballero, A., César, E., Carrera, J., Pérez, J., 2014. Effect of process

parameters and operational mode on nitrous oxide emissions from a nitritation reactor treating reject wastewater. Water Res. 49, 23–33. https://doi.org/10.1016/j.watres.2013.11.009

Ribera-guardia, A., Pijuan, M., 2017. Distinctive NO and N 2 O emission patterns in ammonia oxidizing bacteria : Effect of ammonia oxidation rate , DO and pH. Chem. Eng. J. 321, 358–365. https://doi.org/10.1016/j.cej.2017.03.122

Sabba, F., Picioreanu, C., Boltz, J.P., Nerenberg, R., 2016. Predicting N2O emissions from nitrifying and denitrifying biofilms: a modeling study. Water Sci. Technol. 75, 530–538. https://doi.org/10.2166/wst.2016.484

Sabba, F., Terada, A., Wells, G., Smets, B.F., Nerenberg, R., 2018. Nitrous oxide emissions from biofilm processes for wastewater treatment. Appl. Microbiol. Biotechnol. 102, 9815–9829. https://doi.org/10.1007/s00253-018-9332-7

Schreiber, F., Wunderlin, P., Udert, K.M., Wells, G.F., 2012. Nitric oxide and nitrous oxide turnover in natural and engineered microbial communities : biological pathways , chemical reactions , and novel technologies 3, 1–24. https://doi.org/10.3389/fmicb.2012.00372

Silveira, I.T., Cadee, K., Bagg, W., 2022. Startup and initial operation of an MLE-MABR treating municipal wastewater. Water Sci. Technol. 85, 1155–1166. https://doi.org/10.2166/wst.2022.045

Terada, A., Hibiya, K., Nagai, J., Tsuneda, S., Hirata, A., 2003. Nitrogen removal characteristics and biofilm analysis of a membrane-aerated biofilm reactor applicable to high-strength nitrogenous wastewater treatment. J. Biosci. Bioeng. 95, 170–178. https://doi.org/10.1263/jbb.95.170

Uri-Carreño, N., Eriksen, S., Nielsen, P.H., Andersen, M.H., Hafner, S., Li, Z., Chandran, K., 2017. Continuous aeration control to reduce N2O emissions in a full-scale sidestream deammonification

683 reactor, in: Water Environment Federation Technical Exhibition and Conference 2017, WEFTEC
684 2017. Water Environment Federation, pp. 1211–1219.
685 https://doi.org/https://doi.org/10.2175/193864717822154138

686 Uri-Carreño, N., Nielsen, P.H., Gernaey, K. V., Flores-Alsina, X., 2021. Long-term operation assessment
687 of a full-scale membrane-aerated biofilm reactor under Nordic conditions. Sci. Total Environ. 779,
688 146366. https://doi.org/10.1016/j.scitotenv.2021.146366

689 Uri-Carreño, N., Nielsen, P.H., Gernaey, K. V., Wang, Q., Nielsen, U.G., Nierychlo, M., Hansen, S.H.,
690 Thomsen, L., Flores-Alsina, X., 2022. The effects of low oxidation-reduction potential on the
691 performance of full-scale hybrid membrane-aerated biofilm reactors. Submitt. to Chem. Eng. J.

692 Valkova, T., Parravicini, V., Saracevic, E., Tauber, J., Svardal, K., Krampe, J., 2021. A method to
693 estimate the direct nitrous oxide emissions of municipal wastewater treatment plants based on the
694 degree of nitrogen removal. J. Environ. Manage. 279, 111563.
695 https://doi.org/https://doi.org/10.1016/j.jenvman.2020.111563

696 van Dijk, E.J.H., van Loosdrecht, M.C.M., Pronk, M., 2021. Nitrous oxide emission from full-scale
697 municipal aerobic granular sludge. Water Res. 198, 117159.
698 https://doi.org/10.1016/j.watres.2021.117159

699 Vangsgård, A. K., & Madsen, J. A. (2020). MUDP Lattergaspulje Dataopsamling på måling og reduktion
700 af lattergasemissioner fra renseanlæg. MUDP Rapport [MUDP-The Danish Eco-Innovation
701 Program. N2O Funds. Data Collection on Measurement and Reduction of Nitrous Oxide Emissions
702 from Treatment Plants. MUDP Report], 1–53.

703 Vasilaki, V., Massara, T.M., Stanchev, P., Fatone, F., Katsou, E., 2019. A decade of nitrous oxide (N2O)

monitoring in full-scale wastewater treatment processes: A critical review. Water Res. 161, 392–412. https://doi.org/10.1016/j.watres.2019.04.022

Vasilaki, V., Volcke, E.I.P., Nandi, A.K., van Loosdrecht, M.C.M., Katsou, E., 2018. Relating N2O emissions during biological nitrogen removal with operating conditions using multivariate statistical techniques. Water Res. 140, 387–402. https://doi.org/10.1016/j.watres.2018.04.052

Vogt, L., Luck, M., Biolley, L., Gruber, W., K, L. Von, Kipf, M., Loosli, R., Feller, K., Moosmann, A., Kr, N., Vogel, M., Morgenroth, E., Braun, D., Joss, A., 2021. Estimation of countrywide N 2 O emissions from wastewater treatment in Switzerland using long-term monitoring data Purging pump 13. https://doi.org/10.1016/j.wroa.2021.100122

Weissenbacher, N., Takacs, I., Murthy, S., Fuerhacker, M., Wett, B., 2010. Gaseous nitrogen and carbon emissions from a full-scale deammonification plant. Water Environ. Res. 82, 169–175.

Yan, X., Li, L., Liu, J., 2014. Characteristics of greenhouse gas emission in three full-scale wastewater treatment processes. J. Environ. Sci. 26, 256–263. https://doi.org/10.1016/S1001-0742(13)60429-5